iScience, Volume *25*

Supplemental information

Adipose triglyceride lipase mediates lipolysis and lipid mobilization in response to iron-mediated negative energy balance

Alicia R. Romero, Andre Mu, and Janelle S. Ayres

Supplemental Figure Legends

Supplemental Figure 1. Iron rich diet causes negative energy balance and nutrient malabsorption
Six-week old C57BL/6 males were given control diet (CID) or 2% carbonyl iron diet (IRD) and individually housed in static or metabolic cages in the Comprehensive Laboratory Animal Monitoring System (CLAMS). Weight, gas exchange volumes and food consumption were monitored. (**A**) Absolute body mass over eight-day diet regimen on CID or IRD. Data shown represents two pooled independent experiments (n=11 mice per group). (**B**) Average hourly absolute gas exchange volumes of O_2 consumed and CO_2 respired for mice fed CID or IRD. Data was used to calculate EEJ in **Figure 1B** using modified Weir equation. Data shown represent one independent experiment (n=5-6 mice per group)**.** (**C**) Daily energy expenditure as a function of daily total body mass (TBM) over eight day period (CID linear regression, R^2=.1523, F=8.266, dF=1, 46, P=0.0061, Y = 455.0*X + 29062; IRD linear regression, R^2=.6545, F=71.98, dF=1, 38 , P<0.0001, Y = 1379*X + 6417). Data shown represent analyses of one independent experiment (n=5-6 mice per group). (**D**) Average hourly activity levels plotted as total X directional beam breaks per hour for mice fed CID or IRD in CLAMS and corresponding area under the curve analysis (AUC) for total activity in CLAMS. Data shown represents one independent experiment (n= 6 mice per group) (**E**) Principle component analysis for activity of CID and IRD fed mice in light/dark cycles. Ellipses are indicative of 95% confidence intervals. Data shown represents analyses of one independent experiment (n= 6 mice per group). (**F**) Daily core temperature of CID or IRD fed mice. Data represent two pooled independent experiments (n=5-11 mice per timepoint per group). (**G-L**) C57BL/6 male mice were fed CID *ad libitum* (*ad lib)*, IRD *ad libitum* (*ad lib)*, or CID pair fed matched to average historical IRD food consumption values. (**G**) Absolute body mass over eight-day diet regimens. Data shown represents two pooled independent experiments (n=9 mice per group). Blue asterisks denote comparisons between CID *ad lib* and CID pair fed. Gray asterisks denote comparisons between CID pair fed and IRD *ad lib*. Peach asterisks denote comparisons between CID *ad lib* and IRD *ad lib*. (**H**) Daily core temperature of mice fed CID *ad lib,* pair fed, or IRD *ad lib*. Data represent two pooled independent experiments (n=4-9 mice per timepoint per group). Gray asterisk denotes comparison between CID *ad lib* and CID pair fed. Peach asterisks denote comparisons between CID *ad lib* and IRD *ad lib*. (**I**) Average hourly activity levels plotted as total X directional beam breaks per hour for mice on dietary regimens in CLAMS and corresponding area under the curve analysis (AUC) for total activity in CLAMS. Data shown represents one independent experiment (n= 4 mice per group). (**J**) Principle component analysis for activity mice from three dietary regimens in light/dark cycles. Ellipses are indicative of 95% confidence intervals. Data shown represents analyses of one independent experiment (n= 4 mice per group). (**K**) Average hourly absolute gas exchange volumes of O_2 consumed and CO_2 respired for mice fed CID *ad lib,* pair fed, or IRD *ad lib*. Data was used to calculate EEJ in **Figure 1H** using modified Weir equation. Data shown represent one independent experiment (n=4 mice per group). (**L**) Daily energy expenditure as a function of total body mass (TBM) over eight day period (CID *ad lib* linear regression, R^2=.3360, F=17.2, df= 1, 34, P=0.0002, Y = 565.9*X + 35548; CID pair fed linear regression, R^2=.1905, F=8.002, dF=1, 34 , P=0.0078, Y = 590.3*X + 32039; IRD *ad lib* linear regression, R^2=.8254, F=160.7, dF=1, 34 , P<0.0001, Y = 3300*X - 26401). Data shown represent analyses of one independent experiment (n=4 mice per group). (**M**) Net calorie absorption of mice fed CID and IRD. Data shown represents two time points per diet (Days 4 and 6 post diet initiation). Each data point represents the total caloric intake pooled from two cages of mice minus the total caloric content of solid fecal excrement pooled from the same two cages per respective day of dietary regimen (5 mice per cage, 10 mice pooled). All CLAMS data plotted in zeitgeber time. Data represent mean ±SEM; CID *P<0.05, **P<0.01, ***P<0.001, ****P<0.0001. Related to **Figure 1**.

Supplemental Figure 2. Excess dietary iron causes negative energy balance independent of reduced food intake
C57BL/6 male mice were fed CID *ad libitum* (*ad lib)*, IRD *ad libitum* (*ad lib)*, or CID pair fed matched to average historical iron food consumption values. **(A)** Absolute heart mass and corresponding **(B)** heart mass normalized to total body mass of mice from day eight of pair feeding dietary regimens. Data shown represents 3 pooled independent experiments (n=10-16 mice per group). **(C)** Body composition analyses on day eight of pair fed dietary regimens using Echo MRI. Fat and lean mass were normalized to original body mass. Data shown represents one independent experiment (n=5 mice per group). **(D)** IWAT fat pad mass on day eight of pair feeding dietary regimens normalized to original body mass. Data shown represents one independent experiment (n=5 mice per group). **(E)** Muscle masses on day eight of pair fed dietary regimens normalized to original body mass. Data shown represents one independent experiment (n=4-5 mice per group). (Quadricep; Quad , tibialis anterior; TA, extensor digitorum longus; EDL, soleus, and gastrocnemius; Gastro)**. (F)** Gene

expression in gastrocnemius on day eight of pair fed dietary regimens. Gene expression was normalized to housekeeping expression of *Rps17*. Data shown represents one independent experiment (n=4-5 mice per group). (**G-I**) Mice were housed in the CLAMS to determine the respiratory exchange ratio. (**G**) Average hourly respiratory exchange ratio (RER) calculated as ratio of ml CO_2 OUT (respired):ml O_2 IN (inhaled) and corresponding (**H**) Area under the curve (AUC) analysis for RER for period of matched food consumption. Data shown represents one independent experiment (n=4 mice per group). (**I**) Principal component analysis for the respiratory exchange ratio (RER) of mice in light/dark cycles form the three dietary regimens. Ellipses are indicative of 95% confidence intervals. Data shown represents analyses of one independent experiment (n=4 mice per group). Data represent mean ±SEM; **P*<0.05, ***P*<0.01, ****P*<0.001, *****P*<0.0001. Related to **Figure 2.**

Supplemental Figure 3. Tissue responses to dietary iron supplementation
Six-week old C57BL/6 males were provided control (CID) or 2% carbonyl iron diet (IRD). **(A)** Liver masses from mice fed CID *ad libitum*, CID pair fed, and IRD *ad libitum* for 8 days normalized to respective body mass on day 8 and **(B)** unnormalized raw liver masses**.** Data shown represents three pooled independent experiments (n=10-16 mice per group). **(C)** Circulating levels of alanine amino transferase (ALT) and **(D)** aspartate aminotransferase (AST) in mice fed CID or IRD for nine days. Data shown represents one independent experiment (n=5 mice per group). (**E-H**) Gene expression in (**E**) liver, (**F**) GWAT, (**G**) IWAT, and (**H**) gastrocnemius muscles of mice fed CID or IRD for 6 days. Expression was normalized to *Rps17* expression. Data shown represents one independent experiment (n=5 mice per group). Data represent mean ±SEM. **P*<0.05, ****P*<0.001, *****P*<0.0001. Related to **Figure 3.**

Supplemental Figure 4. Insulin sensitivity not affected by dietary iron supplementation
Six-week old C57BL/6 males were provided control (CID) or 2% carbonyl iron diet (IRD) for a nine-day time course and insulin tolerance tests (ITT) were performed on day 3, 6, and 9 of time course following a 6-hour fast. **(A-D)** ITT curve normalized to basal glucose levels and corresponding area under the curve (AUC) analysis performed on **(A, B)** day 3 and **(C, D)** day 9 post diet initiation. **(E-J)** Absolute glucose levels and corresponding AUC analyses for ITT performed on **(E, F)** day 3, **(G, H)** day 6 and **(I, J)** day 9 post diet initiation. All data shown represents one independent experiment (n=5 mice per group). Data represent mean ±SEM. Related to **Figure 3.**

Supplemental Figure 5. Iron does not influence tissue-level insulin sensitivity
Six-week old C57BL/6 males were provided control (CID) or 2% carbonyl iron diet (IRD) for a nine-day time course and experiments were performed on day 3, 6, and 9 of time course following a 6-hour fast. Mice were injected with insulin and tissues were harvested 15 minutes post injection and snap frozen for analysis. **(A)** Densitometry analyses and **(B)** original blots for AKT activation in GWAT from **Figure 3K**. **(C)** Densitometry analyses and **(D)** original blots for AKT activation in IWAT from **Figure 3L**. **(E)** Densitometry analyses and **(F)** original blots for AKT activation in liver from **Figure 3M**. **(G)** Densitometry analyses and **(H)** original blots for AKT activation in gastrocnemius from **Figure 3N**. All data shown represents one independent experiment. Data represent mean ±SEM; CID n=5, IRD n=5. Related to **Figure 3.**

Supplemental Figure 6: Iron activates lipolysis cascade in white adipose tissue
(A-C) Densitometry quantification of activated proteins in lipolysis pathway from IWAT (**Figure 4A**) normalized to respective total protein and/or housekeeping GAPDH protein. Data shown represents one independent experiment (n= 5 mice per group)**. (D-F)** Densitometry quantification of activated proteins in lipolysis pathway from GWAT (**Figure 4B**) normalized to respective total protein and/or housekeeping GAPDH protein. Data shown represents one independent experiment (n= 5 mice per group). Related to **Figure 4.**

Supplemental Figure 7: Iron activates lipolysis cascade in white adipose tissue (continued)
(A-F) Uncropped Western blot imaging for **Figure 4A** protein extracts from IWAT. (HSL/phospho-HSL Ser563, hormone sensitive lipase; ATGL, Adipose triglyceride lipase; PKA-c, cAMP dependent protein kinase catalytic subunit alpha; GAPDH, Glyceraldehyde3-phosphate dehydrogenase). Data shown represents one independent experiment (n= 5 mice per group)**. (G-L)** Uncropped Western blot imaging for **Figure 4B** protein extracts from GWAT. (HSL/phospho-HSL Ser563, hormone sensitive lipase; ATGL, Adipose triglyceride lipase; PKA-c, cAMP dependent protein kinase catalytic subunit alpha; GAPDH, Glyceraldehyde3-phosphate

dehydrogenase). Data shown represents one independent experiment (n= 5 mice per group). Related to **Figure 4.**

Supplemental Figure 8. Adipose-specific ATGL does not affect net energy balance in response to iron rich diet

Littermate *Pnpla2;Fabp4 cre-* ($Pnpla2^{WT}$) and *Pnpla2;Fabp4 cre+* ($Pnpla2^{WAT\ KO}$) males between six and eight-weeks old were housed in comprehensive laboratory animal monitoring system (CLAMS) metabolic cages for 6 days. Mice were provided 2% carbonyl iron diet (IRD) after brief acclimation period. Daily measurements were taken for body mass, core temperature and food intake. **(A)** Absolute body mass of $Pnpla2^{WT}$ and $Pnpla2^{WAT\ KO}$ mice fed IRD. Data shown represents two pooled independent experiments (n=8-9 mice per group). **(B)** Average hourly absolute gas exchange volumes of O_2 consumed and CO_2 respired for $Pnpla2^{WT}$ and $Pnpla2^{WAT\ KO}$ mice fed IRD. Data was used to calculate EEJ in **Figure 5C** using modified Weir equation. Data shown represents one independent experiment (n=4-5 mice per group)**. (C)** Energy expenditure as a function of total body mass (TBM) over five day period and corresponding **(D)** ANCOVA-predicted EEJ at group average TBM of 21.3 g. Dotted vertical line in regression plot represents group average lean mass ($Pnpla2^{WT}$ linear regression R^2 =.2294, F=6.550, dF= 1, 22, P=0.0179, Y=1311*X+ 14248; $Pnpla2^{WAT\ KO}$ linear regression R^2 =.7201, F=72.05, dF= 1, 28, P<0.0001, Y=1903*X+ 1059; pooled slope=1659) Data shown represents analysis of one independent experiment (n=4-5 mice per group). (**E**) Daily core temperature of $Pnpla2^{WT}$ and $Pnpla2^{WAT\ KO}$ mice. Data represents two pooled independent experiments (n=10-11 mice per group). (**F**) Average hourly activity levels plotted as total X directional beam breaks per hour for $Pnpla2^{WT}$ and $Pnpla2^{WAT\ KO}$ mice fed IRD and corresponding **(G)** Area under the curve (AUC) analysis. Data shown represents one independent experiment (n=4-5 mice per group)**.** (**H**) Principle component analysis for activity of IRD-fed $Pnpla2^{WT}$ and $Pnpla2^{WAT\ KO}$ mice in light/dark cycles. Ellipses are indicative of 95% confidence intervals. Data shown represents analysis of one independent experiment (n=4-5 mice per group). (**I**) Body composition analyses of $Pnpla2^{WT}$ and $Pnpla2^{WAT\ KO}$ mice fed control chow prior to IRD supplementation. Fat and lean mass is normalized to total body mass. Data shown represents one independent experiment (n=4-5 mice per group). Data represent mean ±SEM. Related to **Figure 5.**

Supplemental Figure 1

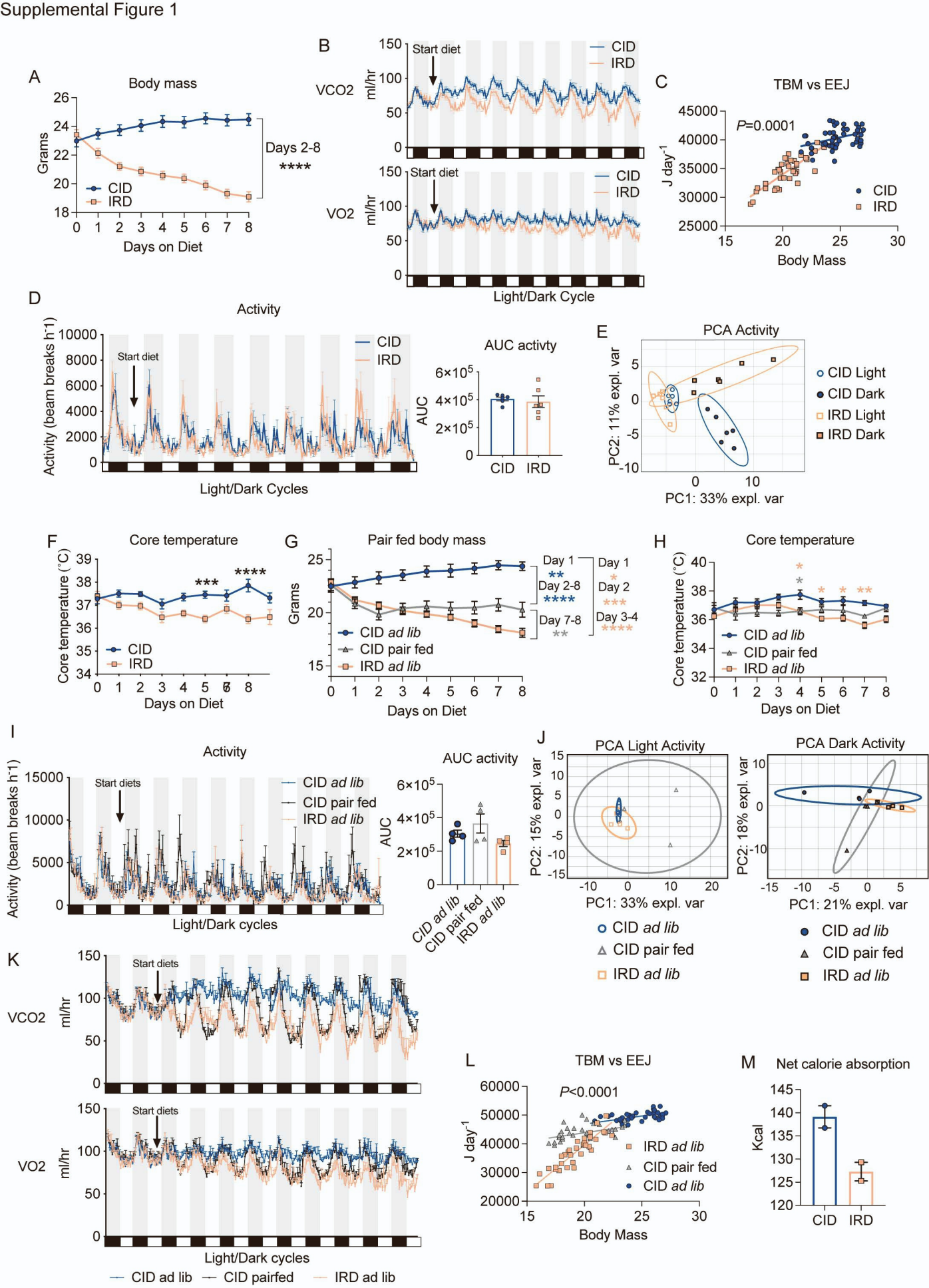

Supplemental Figure 2

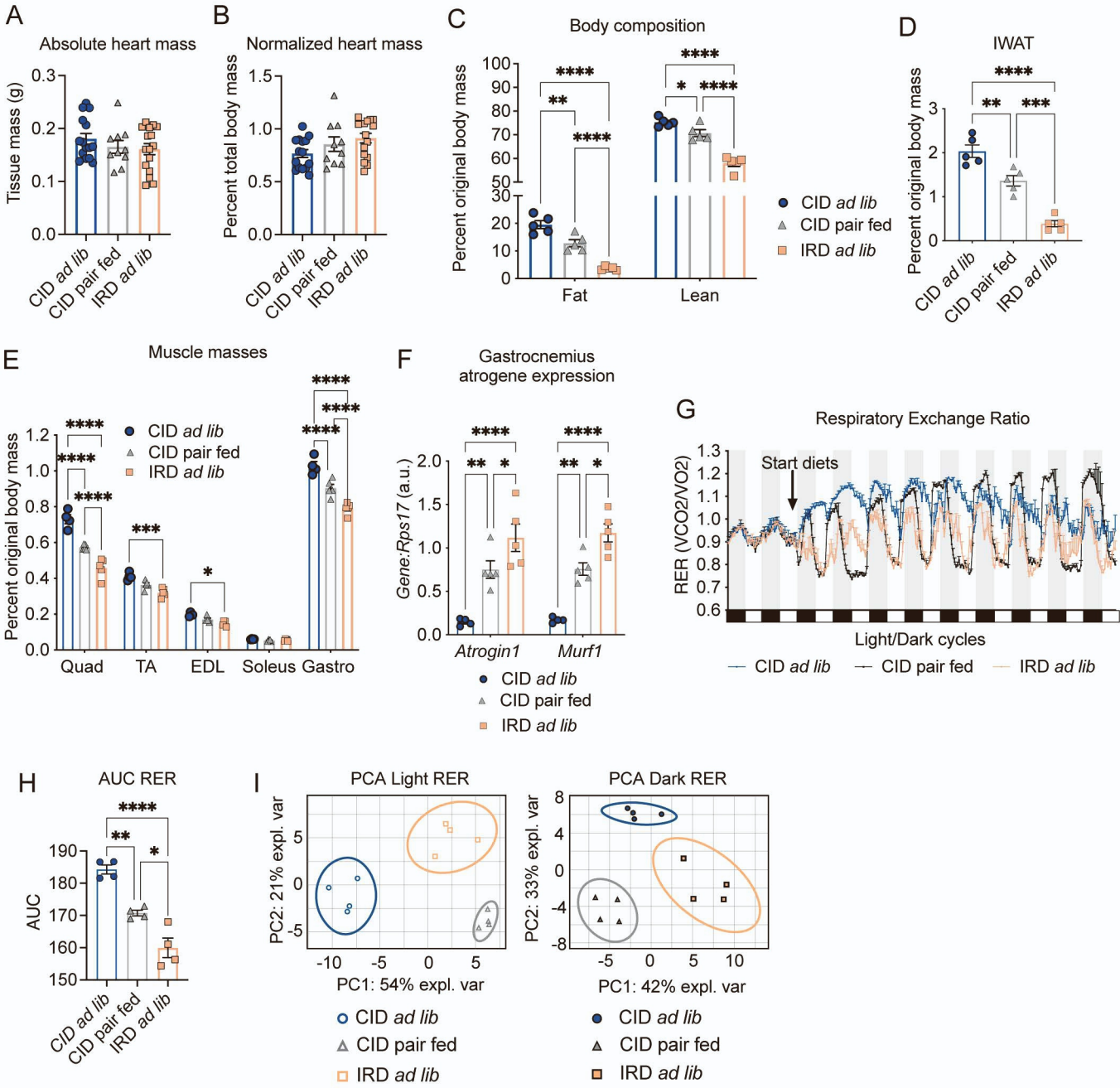

Supplemental Figure 3

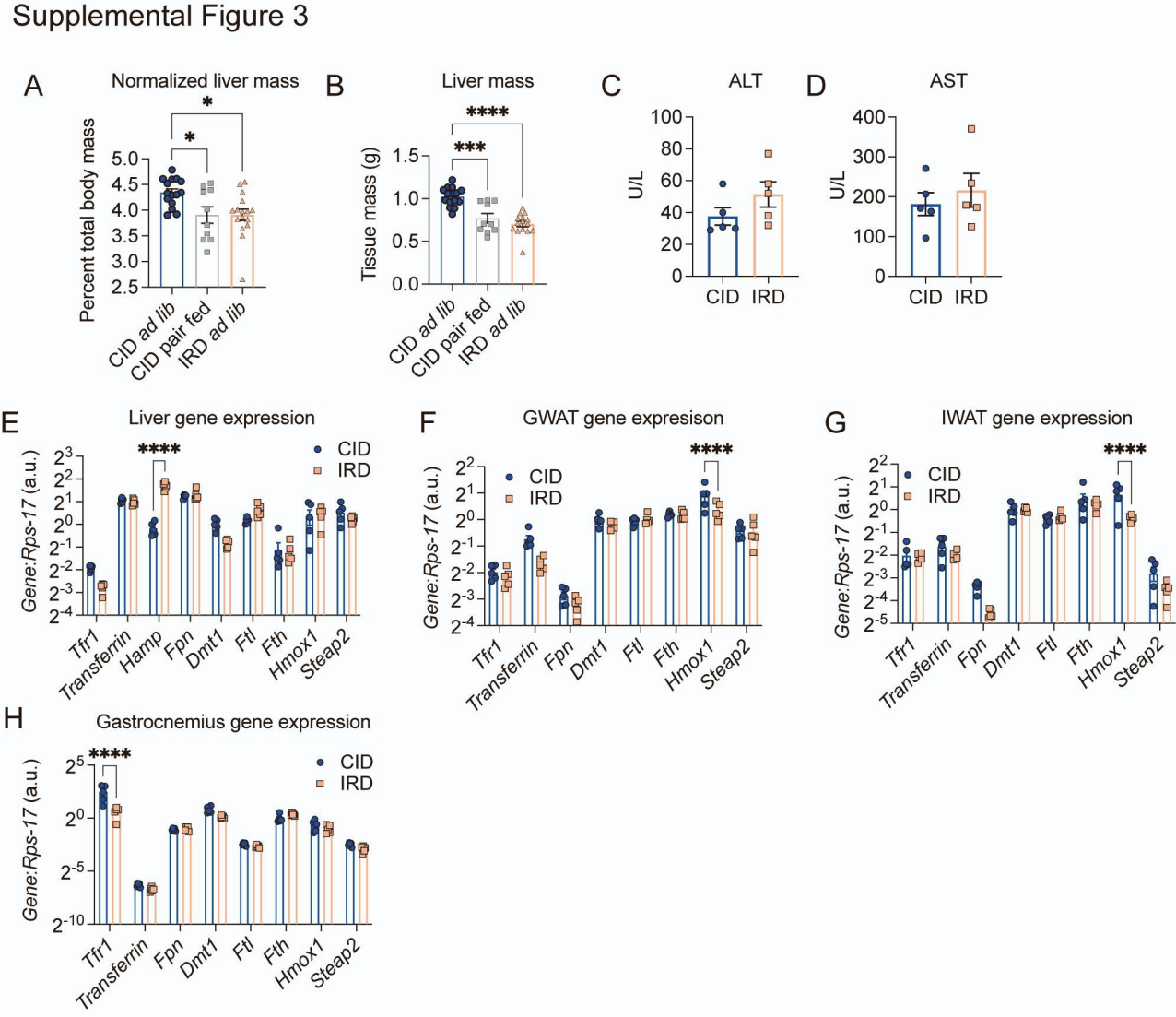

Supplemental Figure 4

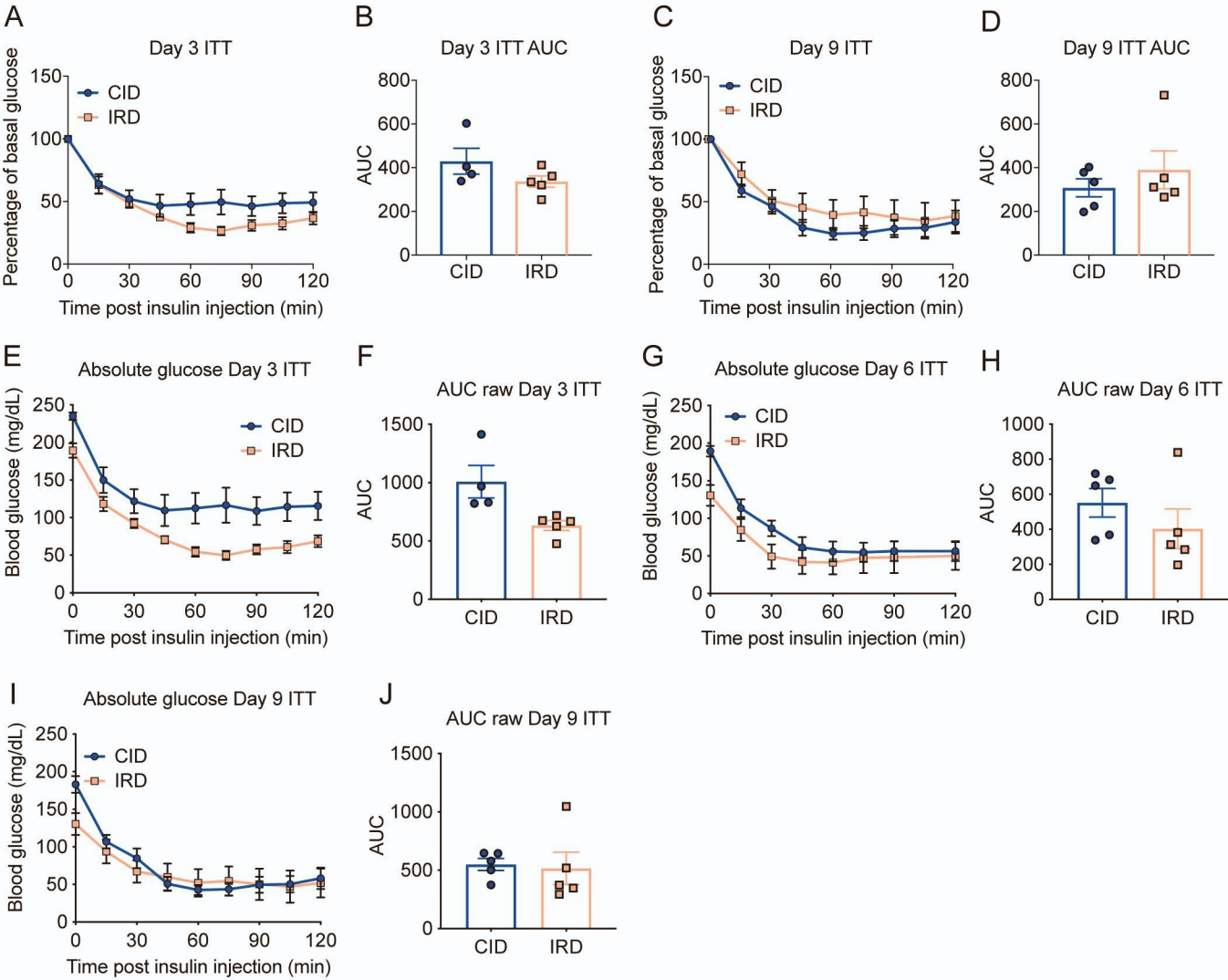

Supplemental Figure 5

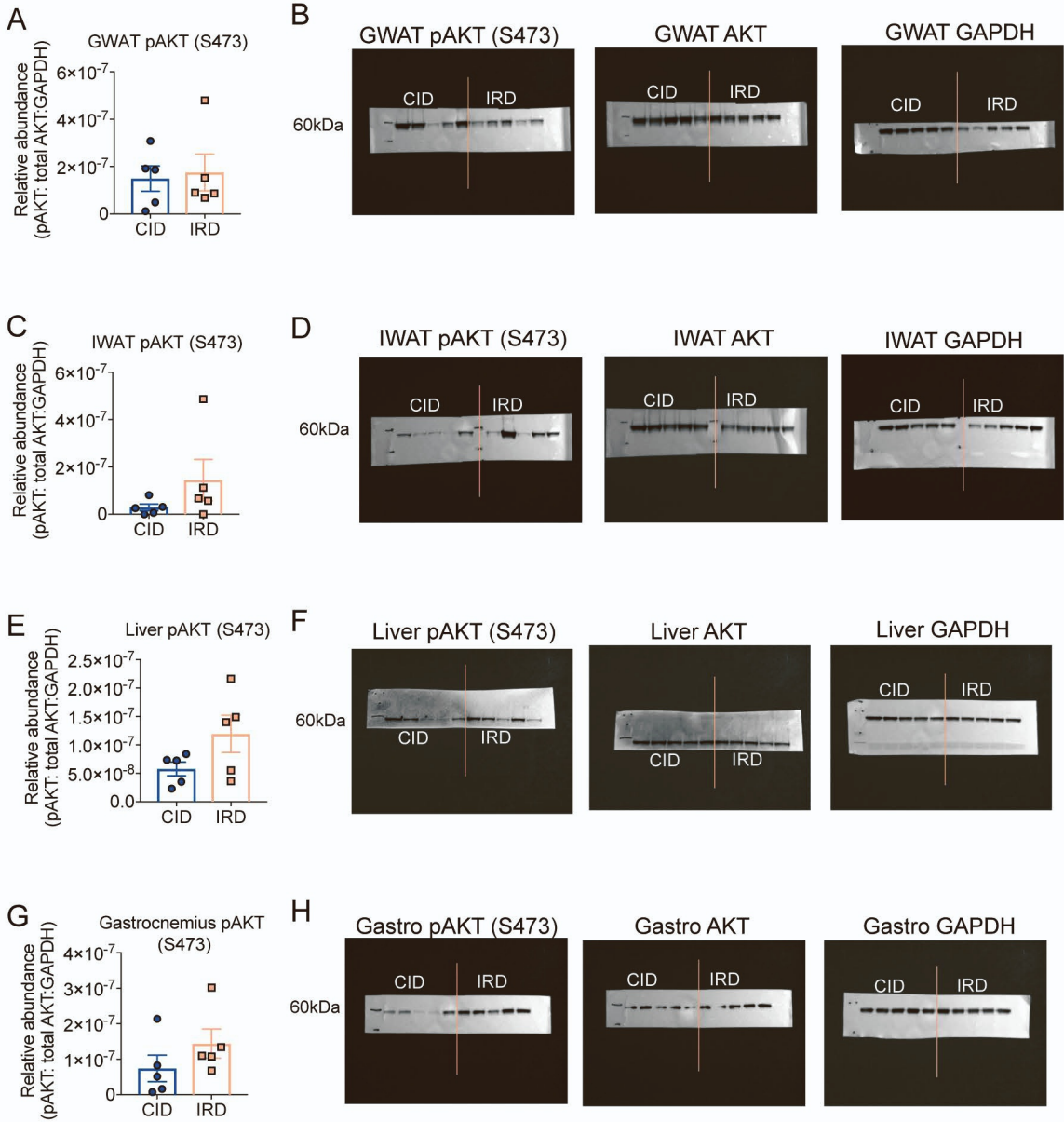

Supplemental Figure 6

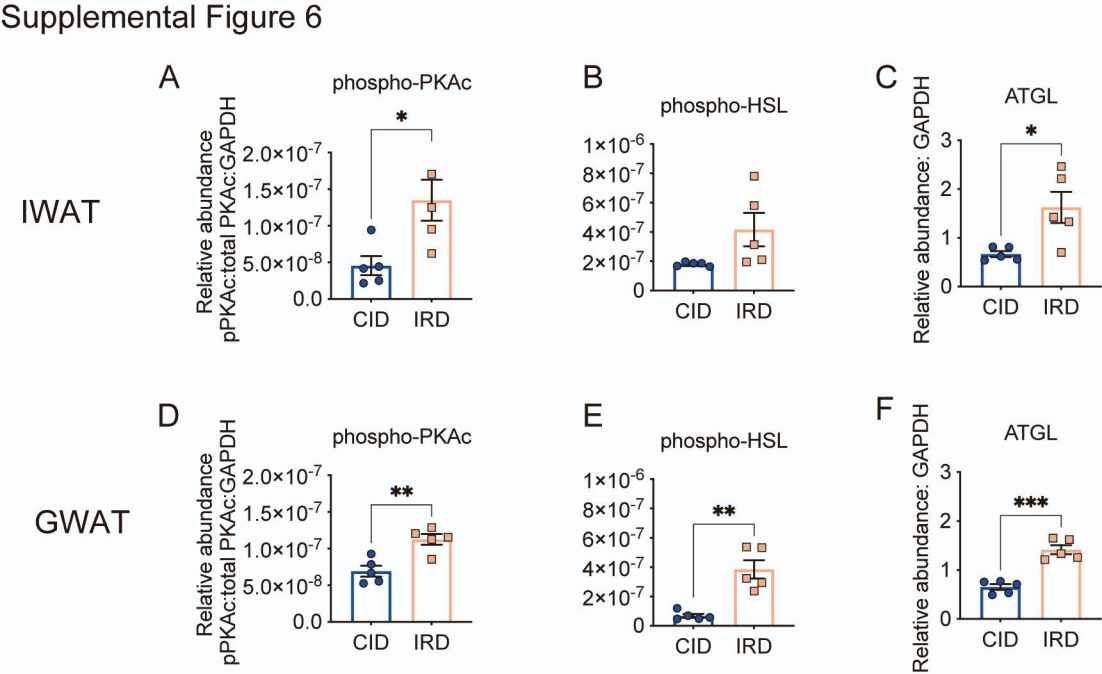

Supplemental Figure 7

A

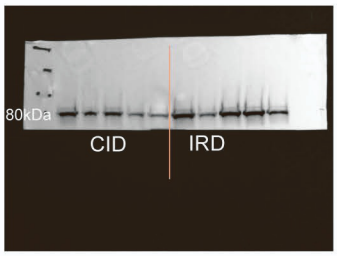

IWAT phospho-HSL (S660)

B

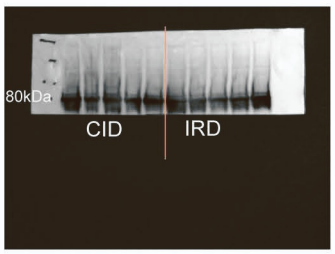

IWAT HSL

C

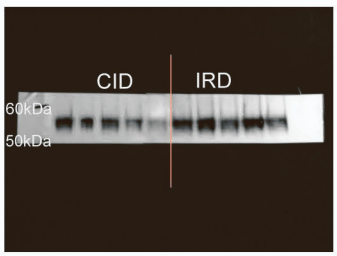

IWAT ATGL

D

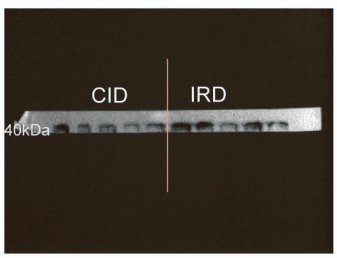

IWAT phospho-PKAc alpha (T197)

E

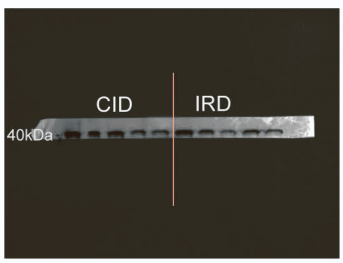

IWAT PKAc alpha

F

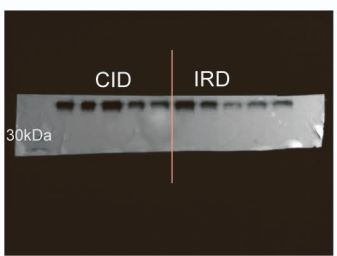

IWAT GAPDH

G

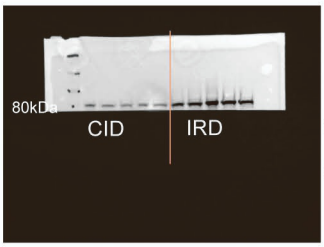

GWAT phospho-HSL (S660)

H

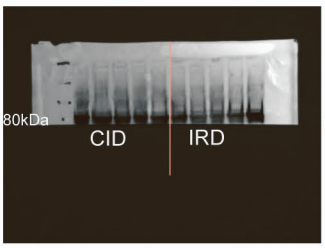

GWAT HSL

I

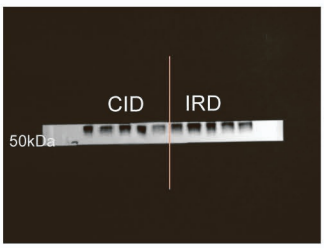

GWAT ATGL

J

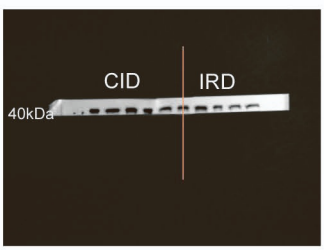

GWAT phospho-PKAc alpha (T197)

K

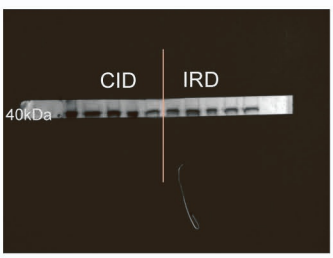

GWAT PKAc alpha

L

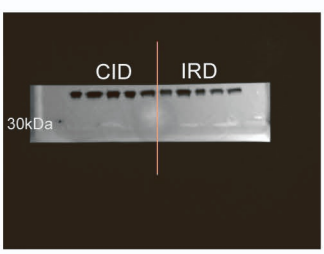

GWAT GAPDH

Supplemental Figure 8